Mon. Not. R. astr. Soc. (1979) **188**, 653–668

Accretion on to highly magnetized white dwarfs

A. R. King and J. P. Lasota* *Astronomy Department, University of Leicester, Leicester LE1 7RH*

Received 1979 January 29; in original form 1978 December 1

Summary. A quantitative theory of accretion on to white dwarfs with magnetic fields of order 10^7–10^8 G is developed. The theory is applied to AM Her and successfully fits X-ray, optical and infrared observations as well as predicting correctly the temporal behaviour of the system.

1 Introduction

Accretion from a close binary companion on to a magnetized white dwarf has for some time been recognized as a possible hard (> 2 keV) X-ray production mechanism. Following the pioneering work of Hoshi (1973) and Aizu (1973), Fabian *et al.* (1976) (see also Katz 1977) were able to produce a consistent picture of this mechanism, paying particular attention to the interaction of the X-rays with the infalling matter. The discovery (Ricketts, King & Raine 1979) of (anti-) correlated hard X-ray and optical behaviour in the dwarf nova SS Cygni, later confirmed by other observers (Fabbiano *et al.* 1978), gives strong qualitative and quantitative support to such models; indeed Ricketts *et al.* were able to estimate the magnetic field ($\sim 10^6$ G) and range of accretion rates ($\sim 4\times10^{16}$ to $\sim 2\times10^{19}$ g/s) by using this theory. The dwarf novae EX Hydrae (Watson, Sherrington & Jameson 1978), U Geminorum (Swank *et al.* 1979; Mason *et al.* 1978) and the old nova GK Persei (King, Ricketts & Warwick 1979) are probably also examples of this type.

This does not, however, exhaust the list of X-ray sources identified with accreting white dwarfs; the outstanding omission is the nova-like variable AM Herculis, which has been detected over a wide energy range. The hard component of the spectrum extends to at least 60 keV (Swank *et al.* 1977) and there is strong soft X-ray emission (e.g. Tuohy *et al.* 1978; Bunner 1978). The large linear and circular optical polarization (Tapia 1976, 1977), which also varies on the 3.1-h binary period, must be due to cyclotron radiation from the accreting gas in a magnetic field of order 10^8 G. This clearly distinguishes AM Her from the other systems mentioned above, which must have magnetic fields at least an order of magnitude weaker.

As explained by Fabian *et al.* (1976), strong cyclotron emission is an efficient coolant of the accretion columns, modifying their structure and the efficiency of X-ray production. In

* On leave from Copernicus Astronomical Center, Polish Academy of Sciences, Warsaw.

this paper we shall give a quantitative treatment of these effects (Section 2), and apply the results to AM Her (Sections 3 and 4). In Section 5 we consider the limitations of the present treatment and discuss further applications.

2 The structure of the accretion columns

The basic physics of the accretion columns for a magnetized white dwarf has been clearly explained by Hoshi (1973), Aizu (1973) and Fabian *et al.* (1976). (See also Masters *et al.* (1977) and Ricketts *et al.* (1979) for modifications and corrections.) We shall therefore recapitulate it only briefly here, emphasizing the difference between our treatment and the earlier ones. We consider throughout a *single* accretion column, for we have in mind applications to models of AM Her-type systems in which the two accretion columns differ markedly in their properties ('slow rotator' models). This accretion is assumed to take place near a magnetic pole of the white dwarf over a small 'cap' of area f' times the white dwarf's surface area of $4\pi R^2 = (4\pi \times 10^{18}\mathrm{cm}^2) R_9^2$, where $R \equiv (10^9\mathrm{cm}) R_9$ is the white dwarf radius. The other accretion column will have cross-sectional area $4\pi R^2 f''$, with $f'' \neq f'$ in general; the maximum value of f' (or f'') is clearly ½, corresponding to spherically symmetric accretion. The radius of the circular cap is $d = 2\sqrt{f'}R$. In the Appendix we give reasons for a particular choice of f' appropriate to AM Her-type objects, and this choice will be used throughout the paper wherever an explicit form is required.

Because of the magnetic channelling of the accretion flow radially on to the white dwarf surface, a standing shock will in general appear over the accretion cap, with shock temperature

$$T_s = 3.7 \times 10^8 M_1 R_9^{-1}\,\mathrm{K} \tag{1}$$

where $M_1 = M/M_\odot$, and M is the mass of the white dwarf. Above this 'strong' shock the material is freely falling; below the shock the density and velocity increase and decrease respectively by a factor of 4. The height D of the shock above the surface is determined by the requirement that the matter should radiate the accretion luminosity

$$L_{\mathrm{acc}} = 1.34 \times 10^{33} M_1 R_9^{-1} F_{16}\,\mathrm{erg/s} \tag{2}$$

(where F_{16} is the accretion rate in units of 10^{16}g/s) from the part of the accretion column below the shock, so that the accreted matter 'settles' on to the surface. Emission from this region takes place via bremsstrahlung and (self-absorbed) cyclotron cooling. The relative importance of these two mechanisms depends on the accretion rate F_{16} and white dwarf magnetic field B. We take the latter equal to the surface field throughout the emission region, whose dimensions are assumed small compared with R, and write $B = 10^8 B_8$G, since we expect fields of this order for AM Her objects. *If F_{16} is sufficiently large compared to B_8*, cyclotron cooling will be relatively inefficient and the electrons will reach the shock temperature T_s and radiate predominantly by bremsstrahlung. (We assume for simplicity a uniform temperature and density in the radiating region. This is an adequate approximation for our purposes; a solution of the flow is given by Aizu (1973). In this situation, which we call case (a) we may define a parameter a as the ratio of free–free to cyclotron luminosities: since the sum of these two must equal L_{acc} we have

$$L_{\mathrm{ff}} = aL_{\mathrm{cyc}} = \frac{a}{a+1} L_{\mathrm{acc}}. \tag{3}$$

To calculate L_{ff} we assume the accretion flow is radial and uniform; hence above the shock, where the matter has the free-fall velocity $v(r) = (2GM/r)^{1/2}$, the density of the accre-

tion column is

$$\rho = \frac{F}{4\pi R^2 f' v(r)}.$$

Since ρ increases four-fold at the shock, we find for the electron density below the shock

$$N_e = 5.7 \times 10^{12} F_{16} f'^{-1} M_1^{-1/2} R_9^{-3/2} \text{ cm}^{-3} \quad (4)$$

assuming a mean molecular weight of 0.615 for the accreting material. With a free–free emissivity $j_{ff} = 2 \times 10^{-27} N_e^2 T_s^{1/2} \text{ erg s}^{-1} \text{ cm}^{-3}$ one can calculate the bremsstrahlung luminosity

$$L_{ff} = 4\pi R^2 f' D j_{ff}. \quad (5)$$

With the useful definition

$$\phi = 1 + \frac{2D}{d} = 1 + \frac{D f'^{-1/2}}{R} \quad (6)$$

we find

$$L_{ff} = 1.59 \times 10^{31} F_{16}^2 f'^{-1/2} M_1^{1/2} R_9^{-1/2} (\phi - 1) \text{ erg/s}. \quad (7)$$

With our adopted value (see Appendix)

$$f' = 5.18 \times 10^{-4} F_{16}^{2/7} B_8^{-4/7} M_1^{1/7} R_9^{-5/7}$$

we get finally

$$L_{ff} = 7.11 \times 10^{32} F_{16}^{13/7} B_8^{2/7} M_1^{-4/7} R_9^{-1/7} (\phi - 1) \text{ erg/s}. \quad (8)$$

Following earlier authors (e.g. Masters *et al.* (1977), Chanmugam & Wagner (1978)) we assume that the self-absorbed cyclotron radiation produces a Rayleigh–Jeans spectrum at the electron temperature T_e up to some harmonic m_* of the cyclotron frequency

$$\nu_c = 2.8 \times 10^{14} B_8 \text{ Hz}.$$

Above frequencies $m_* \nu_c$, the opacity is assumed so low that the emission is negligible. Thus the cyclotron luminosity is

$$L_{cyc} = \frac{A 2\pi k T_e m_*^3 \nu_c^3}{3c^2}$$

where A is the emitting area. From the definition of f' and equation (6) this is $4\pi R^2 f' \phi$, so in case (a), where $T_e = T_s$, we find

$$L_{cyc} = 1.6 \times 10^{31} F_{16}^{2/7} B_8^{17/7} M_1^{8/7} R_9^{2/7} m_*^3 \phi. \quad (9)$$

In this paper we shall regard m_* as an observationally determined parameter, ignoring its likely dependence on F_{16} and B_8. This aspect of the theory is somewhat unsatisfactory, and one cannot be very confident that the true, self-absorbed cyclotron spectrum will be a pure Rayleigh–Jeans – indeed the observed spectrum of AM Her is rather flatter (e.g. Priedhorsky & Krzemiński 1978); however, it is mainly the total luminosity L_{cyc} which will concern us here, and it is not unreasonable to suppose that equation (8) represents a fair estimate.

For case (a), equations (2), (3), (8) and (9) give five relations to determine the five unknowns L_{acc}, L_{ff}, L_{cyc}, ϕ and a in terms of F_{16} and B_8, assuming M_1, R_9 and m_* known. Thus we may plot an F–B plane for each set of values M_1, R_9, m_* in the manner of Fabian *et al.* (1976) and Ricketts *et al.* (1979). In those papers the equations were solved in the

asymptotic regions $\phi = 1$ and $\phi \gg 1$, corresponding to $D \ll d$ and $D \gg d$ respectively. There result simple power-law dependences for all quantities. However, we shall see that AM Her in particular lies awkwardly in regions $1 < \phi \lesssim 10$ of the F–B plane where the asymptotic solutions can be seriously misleading; hence in this paper the full set of equations will be solved simultaneously.

In order to get a complete F–B diagram we must also consider the case where cyclotron cooling is so efficient that the electrons never reach the shock temperature T_s: this we call case (b), and to make clear which case is being discussed we define a parameter b by the analogous equations to (3):

$$L_{ff} = bL_{cyc} = \frac{b}{b+1} L_{acc}. \tag{10}$$

In these equations L_{ff}, L_{cyc} must now be calculated using the electron temperature T_e in place of T_s. Hence L_{ff} in equation (8) has to be multiplied by $(T_e/T_s)^{1/2}$ and L_{cyc} in equation (9) by T_e/T_s. In order to close the system of equations in this case we need a further relation for T_e: this comes from the requirement that collisional heating of the electrons by the ions balance cyclotron losses (Fabian *et al.* 1976). Thus

$$L_{cyc} = 4\pi R^2 f' D j_c$$

where $j_c = 2.7 \times 10^{-18} N_e^2 T_s T_e^{-3/2}$ erg s^{-1} cm^{-3} is the collisional heating rate. Comparing these equations with equation (5) and using the first of equations (10) gives immediately a useful relation between b and T_e:

$$\left.\begin{aligned} b = \frac{L_{ff}}{L_{cyc}} = \frac{j_{ff}}{j_c} &= 2 \times 10^{-18} T_e^2 M_1^{-1} R_9 \\ \text{or} \\ T_e &= 7.1 \times 10^8 b^{1/2} M_1^{1/2} R_9^{-1/2}. \end{aligned}\right\} \tag{11}$$

The border between the case (a) and (b) regions in the F–B plane is the curve on which T_e calculated in this way equals the shock temperature T_s, so here

$$b = b_{max} = 0.27 M_1 R_9^{-1}. \tag{12}$$

Clearly, on this curve $a = b =$ constant, for the first of equations (10) may be in general written

$$bL_{cyc}(T_s) = \left(\frac{T_s}{T_e}\right)^{1/2} L_{ff}(T_s),$$

using the fact that $L_{cyc}(T_e) \propto T_e$, $L_{ff}(T_e) \propto T_e^{1/2}$. This relation goes over into the first of equations (3) on $T_e = T_s$ provided a equals the value of b given by equation (12).

We are now in a position to solve the equations in cases (a) and (b). The procedure for both sets is to obtain the curves in the F–B plane on which a (or b) is constant. These are

$$2aF_{16}^{-11/7} B_8^{15/7} M_1^{12/7} R_9^{3/7} + (a+1) F_{16}^{-5/7} B_8^{17/7} M_1^{1/7} R_9^{9/7} = 100 m_*^{-3} \tag{13}$$

and

$$3b^{5/4} F_{16}^{-11/7} B_8^{15/7} M_1^{41/28} R_9^{19/28} + 2b^{1/2}(b+1) F_{16}^{-5/7} B_8^{17/7} M_1^{-5/14} R_9^{25/14} = 100 m_*^{-3}. \tag{14}$$

It may easily be checked that the two curves are identical for $a = b = b_{max}$ ($T_e = T_s$). In the large $-F_{16}$ regime we have $F_{16} \propto B_8^{17/5}$ in both cases; this corresponds to the region $\phi \sim 1$.

For small F_{16}, we have $F_{16} \propto B_8^{15/11}$, which is the region $\phi \gg 1$. These asymptotes, which are of course straight lines in the $\log F$–$\log B$ plane, are the lines plotted by earlier authors; they were there arbitrarily assumed to intersect on some curve $\phi \approx 2$.

With the curves a = constant, b = constant plotted on the $\log F$–$\log B$ plane, one may readily plot other curves of interest. The curves $L_{\rm ff}$ = constant follow immediately from equations (3) and (10) which imply that

$$F_{16} = 7.52 \times 10^{-34} \left(1 + \frac{1}{a}\right) L_{\rm ff} M_1^{-1} R_9 \tag{15}$$

in the (a) region, with a replaced by b in the (b) region. Thus given a value of $L_{\rm ff}$, equation (15) yields the value of F_{16} on each curve a or b = constant. To find the position of the shock above the surface we compute D/R from equation (5). We find

$$D/R = 3.27 \times 10^{-35} L_{\rm ff} F_{16}^{-12/7} B_8^{-4/7} M_1^{9/14} R_9^{-3/14}. \tag{16}$$

This gives the value of D/R at any point whose parameters (F, B, a, etc.) are known, and we may also use it to plot the curves D/R = constant. For example, the curve $D/R = 1$ intersects the curve $L_{\rm ff} = 10^{33}$ where $F_{16} = 0.14 B_8^{-1/3} M_1^{3/8} R_9^{-1/8}$. The intersection point is then easily found either numerically or graphically. Occasionally it is more convenient to get D/R from equations (6) and (9), which in any case gives a useful consistency check. The value of ϕ, which gives the relative dimensions D/d of the shocked region of the accretion column follows in case (a) from $L_{\rm ff} = a/(a+1)\, L_{\rm acc}$, equations (2) and (8). We find.

$$\phi = 1 + \frac{1.88a}{a+1} F_{16}^{-6/7} B_8^{-2/7} M_1^{11/7} R_9^{-6/7}. \tag{17}$$

In case (b) it is more accurate to use $L_{\rm cyc} = (1+b)^{-1} L_{\rm acc}$, giving

$$\phi = \frac{41.25}{b^{1/2}(b+1)} F_{16}^{5/7} B_8^{-17/7} M_1^{5/14} R_9^{-25/14} m_*^{-3}. \tag{18}$$

Using the known curves a, b = constant we now get the point of intersection of the curves ϕ = constant with these curves either numerically or graphically. For small F_{16} in the (b) region we find from equation (14) $b \propto F_{16}^{44/35} B_8^{-12/7}$, so using equation (18) we see that $F_{16} \propto B_8^{55/3}$ on ϕ = constant for small F_{16}. This means that the ϕ = constant curves actually bend back slightly to lower values of B_8 as F_{16} is reduced.

Finally one may plot on the $\log F$–$\log B$ plane lines specifying photoelectric absorption and degradation by inelastic electron scattering of any X-rays that pass through the cooler material above the shock in the accretion columns (Fabian *et al.* 1976; Ricketts *et al.* 1979). One finds easily that the X-rays encounter a column density

$$N = 2 \times 10^{21} F_{16} f'^{-1/2} M_1^{-1/2} R_9^{-1/2}\ {\rm cm}^{-2}$$

as they leave through the sides of the column (as they must, since its height is greater than its width d). With an effective photoelectric absorption cross-section $\sigma = 4 \times 10^{-22} E^{-3}\,{\rm cm}^2$ for photons of energy E keV one finds

$$\tau_{\rm pe}(E) = 0.8 E^{-3} F_{16} f'^{-1/2} M_1^{1/2} R_9^{-1/2} = \frac{\sigma}{\sigma_{\rm T}} \tau_{\rm es}$$

where $\tau_{\rm pe}(E)$, $\tau_{\rm es}$ are the photoelectric and electron scattering optical depths and $\sigma_{\rm T}$ is the Thomson cross-section, and we have assumed that the keV-absorbing atoms have retained their K-shell electrons (Fabian *et al.* 1976). With our choice of f' the photoelectric

absorption has optical depth unity for photons of energy E on the line

$$F_{16} = 1.54 \times 10^{-2} B_8^{-1/3} E^{7/2} M_1^{2/3} R_9^{1/6}. \tag{19}$$

On this line τ_{es} has the constant value

$$\tau_{es} = 1.68 \times 10^{-3} E^3. \tag{20}$$

Of course if D/d is large, most of the X-ray flux (if any) from the shocked gas will escape through the sides of the shocked region rather than first upwards through the shock. It will therefore suffer little photoelectric absorption as the keV-absorbing atoms in the shocked region will not have retained their K-shell electrons. However, provided ϕ is not very much larger than about 3 the X-ray spectrum will still show a photoelectric low-energy turnover corresponding to $\tau_{pe} \approx 1$.

Figs 1, 2 show $\log F$–$\log B$ planes for two choices of parameters:

Fig. 1: $M_1 = 1$, $R_9 = 0.53$, $m_* = 3$,
Fig. 2: $M_1 = 1$, $R_9 = 0.53$, $m_* = 5$.

(These choices are made with applications to AM Her in mind; however, the qualitative features they exhibit are common to all diagrams.) Note that from equation (11), X-ray emission at $kT \geqslant 2$ keV is only possible provided

$$b > b_{\min} = 1.07 \times 10^{-3} M_1^{-1} R_9. \tag{21}$$

The curve $b = b_{\min}$ is also plotted in Figs 1 and 2.

It is worth noting also that the curve $D/R = 1$ does not intersect the line $\tau_{es} = 1$ for reasonable values of the parameters: one can easily show that they meet only in regions $B_8 \lesssim 10^{-6}$, i.e. fields of a few hundred gauss or less. This is in agreement with the result of Kylafis & Lamb (1979), obtained for spherical accretion on to unmagnetized white dwarfs.

3 Application to AM Her

We can now use the $\log F$–$\log B$ planes described in the last section to try to deduce a consistent set of parameters for the accretion columns of AM Her. At the outset, we must distinguish between two classes of models: the 'fast' and 'slow' rotators. In fast rotator models (e.g. Fabian *et al.* 1977) the usual picture of a cataclysmic variable is adopted; an accretion disc is assumed to form around the white-dwarf primary, with a 'hot-spot' where the gas stream from the late-type secondary meets the disc. The accretion of angular momentum by the white dwarf causes it to spin up, hence the label 'fast' rotator. In Fabian *et al.*'s (1977) qualitative model, a combination of reflection and scattering effects by the disc and hot-spot is proposed to explain the observed light curves and phase-dependent polarizations. In slow rotator models (e.g. Priedhorsky & Krzemiński 1978; Stockman *et al.* 1977; Chanmugam & Wagner 1978) the white dwarf is assumed to spin synchronously with the orbital period; no real accretion disc forms because of the high magnetic field of the white dwarf (see Appendix). Almost all the observed radiation, from infrared to X-ray, is supposed to be produced in accretion columns close to the white dwarf's magnetic poles, and it is the body of the white dwarf itself which produces dips in the various light curves. In some models (e.g. Chanmugam & Wagner 1978) there is significant accretion only on to the white dwarf pole facing the secondary; in most slow rotator models the two poles are assumed

asymmetric in both magnetic field and accretion rate. For our purposes the important point is that the two-pole slow rotator models impose more constraints on the accretion columns: we must find two slightly differing sets of parameters $(F_{16}, B_8 m_*)$ which give the (fairly divergent) observed behaviour of the two poles of the white dwarf required in these models; and of course we must keep M_1, R_9 the same for the two poles. In the single-pole slow rotator and fast rotator models there is only one, or one kind of, accretion column to describe, so this part of the problem follows *a fortiori* if we can solve it for the two-pole models. We do not choose here to discuss other constraints on the single-pole and fast rotator

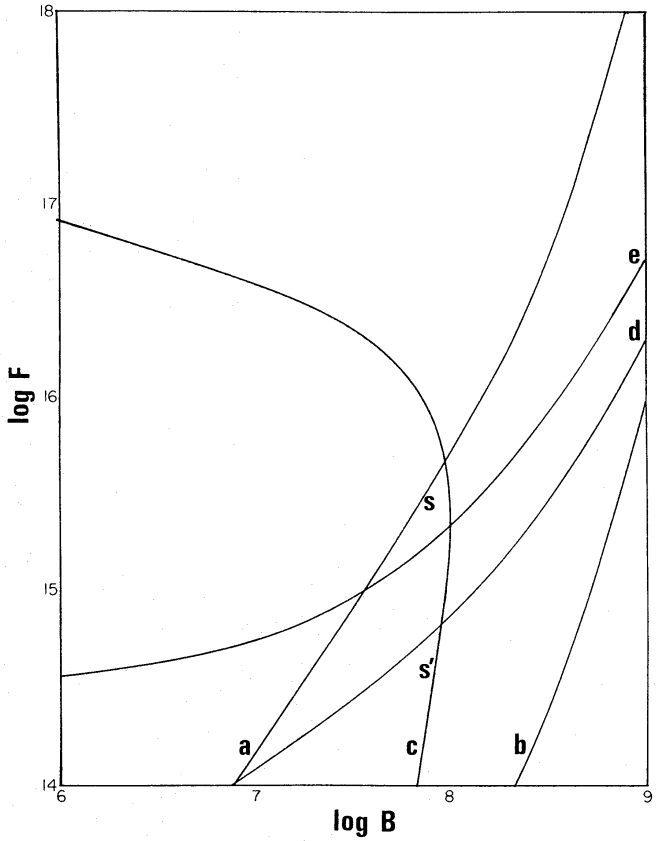

Figure 1. The dependence on accretion rate F g/s and magnetic field B(G) of various properties of the accretion column in a white dwarf of $1M_\odot$, with radius 5.3×10^8 cm. The cyclotron emission is assumed self-absorbed up to a frequency three times the fundamental ($m_* = 3$). Curves (a–e) represent the following: (a) On this curve the electron temperature T_e, calculated under the assumption that collisional heating by the ions balances cyclotron losses, actually equals the shock temperature T_s of the ions. To the right of this curve $T_e < T_s$ (case (b)); to the left $T_e = T_s$ (case (a)). (b) On this curve $kT_e = 2$ keV, so hard X-rays are not emitted for (F, B) values to the right of it. (c) Here the height D of the shock-heated part of the accretion column equals its radius d ($\phi = 3$). Above and to the right of this curve, $D \ll d$ ($\phi \approx 1$), while in the bottom left corner of the diagram $D \gtrsim d$ ($\phi > 1$). (d) The free–free luminosity from the column (mostly emitted as hard X-rays) has the constant value $L_{ff} = 10^{31}$ erg/s. (e) The same as curve (d), but with $L_{ff} = 3 \times 10^{31}$ erg/s. In applying this diagram to the study of the strong magnetic pole of AM Her, the observational data imply that the system point lies near the vertical line $B \approx 7 \times 10^7$ G. There is little hard X-ray emission from this pole, so that a case (b) solution is probably required, fixing the upper limit to the system point's position at about S, where $L = 1.4 \times 10^{32}$ erg/s. A precise determination of the total cyclotron luminosity by optical and IR observations is needed to fix the position of the system point in, e.g. an optical high state: a lower limit is probably given by point S′, where $L_{cyc} = 1 \times 10^{32}$ erg/s. At all points on the line SS′ the column height D is of order one-tenth of the white dwarf radius, so the emission region can be efficiently eclipsed by the body of the white dwarf, as required for self-consistency of slow-rotator models.

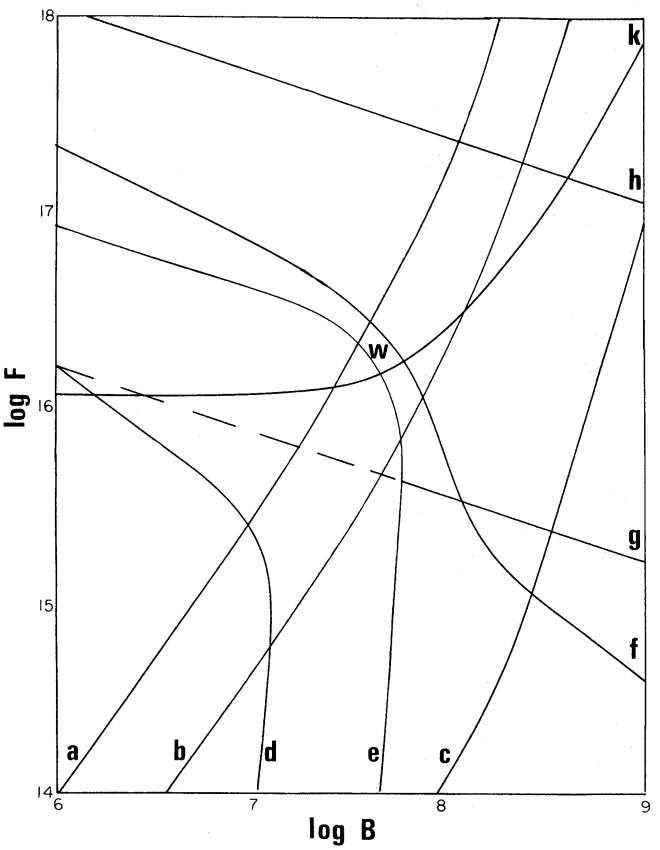

Figure 2. A similar diagram to Fig. 1, with the white dwarf mass ($1M_\odot$) and radius (5.3×10^8 cm) unchanged, but with cyclotron emission assumed self-absorbed up to a frequency five times the fundamental ($m_* = 5$). Curves (a–k) are as follows: (a) On this curve the free–free luminosity of the column is 10 times its cyclotron luminosity ($a = 10$). (b) As on curve (a) of Fig. 1. The shocked column's electron temperature T_e = the shock temperature T_s. (c) As on curve (b) of Fig. 1. $kT_e = 2$ keV here. (d) On this curve the shock height D equals the white dwarf radius R. Thus an acceptable solution providing for substantial eclipses of the pole by the white dwarf's body must give a system point lying either above or to the right of this curve, where $D < R$. (e) As for curve (c) of Fig. 1, the shock height D equals the accretion column radius d here ($\phi = 3$). (f) On this curve the blackbody temperature T_b, calculated on the assumption that hard X-rays from the accretion columns intercepted by the white dwarf atmosphere are completely thermalized, has the constant value 2.8×10^5 K. This is the lowest value compatible with the observations of Tuohy *et al.* (1978). Below *f*, T_b decreases further. In Section 4 we give our reasons for doubting this assumption. (g) On this line 2.5 keV X-rays encounter unit photoelectric optical depth (τ_{pe} (2.5 keV) = 1) in escaping through the cooler part of the accretion column above the shock. For $\phi > 3$ much of this flux leaves directly from the hotter, shocked, emission region where the keV-absorbing elements will have lost their K-shell electrons; for this reason the line is shown dotted for $\phi > 3$. τ_{pe} increases as F is increased. (h) Here the electron scattering optical depth through the sides of the accretion column is unity. For points below this line, $\tau_{es} < 1$ and the escaping X-rays are not degraded by Compton scattering. (k) As for curves (d) and (e) of Fig. 1: here $L_{ff} = 3\times10^{33}$ erg/s. Point W represents a possible solution for the weak magnetic pole in an optical high state. With $m_* = 5$ observation requires $B = 4\times10^7$ G, and the estimated $L_{ff} \approx 6L_{cyc}$ leads to point W, which is the intersection of the curve $a = 6$ with the line $B_8 = 0.4$. Here the predicted luminosities agree with observation provided the system's distance is about 150 pc. The predicted photoelectric cut-off ($\tau_{pe} = 1$ for ~ 3 keV) is also in fair agreement with the observed ~ 2.5 keV cut-off (Swank *et al.* 1977). At W, D/R is of order 0.1, allowing efficient eclipses by the white dwarf body. Other slightly different solutions are possible depending on the precise parameters adopted for the system (see Section 3).

models which may tend to favour the two-pole models (see, e.g. Priedhorsky & Krzemiński 1978; Angel 1978; Kruszewski 1978).

The observational data on AM Her have been ably summarized by Kruszewski (1978). As shown in this paper, in two-pole slow rotator models the X-rays must be produced at the pole having the smaller magnetic field of the two ('the weak pole'). This pole must also dominate in the near infrared because the cyclotron frequency of the other ('strong') pole is assumed to lie in the optical. All this agrees with the observed facts that the optical secondary minimum coincides with the X-ray eclipse (Swank *et al.* 1977) and the deeper minimum at 2.2 μm (Jameson *et al.* 1978; see also Neugebauer *et al.* 1979). The strong pole's cyclotron radiation dominates the optical light and is eclipsed at optical primary minimum, but this pole produces no X-rays, presumably because of the cyclotron cooling.

We shall show here that this picture can be made quantitatively reasonable, in that a consistent set of parameters for the two poles can be found. We consider first the strong pole, for which the lack of cyclotron emission outside the range 4500–15 000 Å (Kruszewski 1978) implies

$$B_8 \approx 0.7, \quad m_* \approx 3. \tag{22}$$

The mass of the white dwarf must be more than about $0.9\,M_\odot$ in order to give the observed X-ray temperature $kT \gtrsim 60$ keV (Swank *et al.* 1977) for the weak pole. (But see the discussion of the results of Staubert *et al.* (1978) later in this section.) For white dwarf masses near the Chandrasekhar limit of $1.4\,M_\odot$ the shock temperature and accretion luminosity become so high that very small values of b are required to reduce the predicted X-ray flux from the strong pole to a value compatible with the X-ray light curves (*cf.* equations (2), (10) and (11)). Such small values of b inevitably lead to magnetic fields in excess of 10^9 G, which of course violates equation (22). Thus the white dwarf mass must be quite close to $1M_\odot$, and we adopt $M_1 = 1$, $R_9 = 0.53$ in the following. We must therefore determine a region in the $\log F$–$\log B$ plane of Fig. 1, in which the strong pole may lie subject to the constraints of the observations. First, equation (22) means that the point representing the strong pole must lie on or near the vertical line $B_8 = 0.7$. The other constraints come from the cyclotron and X-ray luminosities which may be inferred from observation for this pole. Since one-half of any radiation from the shocked column will be emitted downwards and thermalized in the white dwarf atmosphere (see Section 4) the *emitted* cyclotron luminosity $L_{\rm cyc}$ will be *twice* the observed optical and infrared luminosity of the strong pole; in the optical high state it is thus of order $(1\text{–}3) \times 10^{32} D_{100}^2$ erg/s, where D_{100} is the distance to the system in units of 100 pc, and we expect $D_{100} \gtrsim 1$ (see, e.g. Swank *et al.* 1977). Any point on the line $B_8 = 0.7$ which is in case (b) has F_{16} of order 0.1 or less, implying $L_{\rm ff}$ of order 10^{32} erg/s or less (which means an X-ray luminosity of one-half of this value). This is small compared to the observed 2–60 keV luminosity of $9 \times 10^{32} D_{100}^2$ erg/s (Swank *et al.* 1977) and so is fully consistent with the single total eclipse in the X-ray light curve. The upper limit to the position of the 'system point' on the line $B_8 = 0.7$ is probably given by point S, where $F_{16} = 0.3$, implying $L_{\rm X} = 0.5\,L_{\rm ff} = 1.4 \times 10^{32}$ erg/s and $L_{\rm cyc} = 5.2 \times 10^{32}$ erg/s; of course a precise determination of the total observed cyclotron emission from this pole is needed to fix its position on the line $B_8 = 0.7$. A lower limit to the position is probably given by point S′, for which $L_{\rm cyc} = 1 \times 10^{32}$ erg/s. At a representative point on the line SS′, the parameters of the strong pole are $D/R \approx 0.1$, $\phi = 8$, $kT_{\rm e} = 32$ keV. The last quantity of course varies up to 64 keV for S, but the other two are essentially constant on SS′. The value of D/R means that the model is self-consistent, in that the emission region can be efficiently eclipsed by the body of the white dwarf.

For the weak pole, the analogous limits to equation (22) are

$$B_8 \lesssim 0.4, \quad m_* B_8 \approx 2. \tag{23}$$

Infrared polarimetry, which may be possible from UKIRT, is necessary to fix an exact lower limit to B_8, but we do not anticipate B_8 much smaller than 0.4 as $B_8 = 0.7$ for the other pole. Thus we expect $5 \lesssim m_* \lesssim 8$. For $M_1 = 1$, $R_9 = 0.53$, which we must adopt again, the shock temperature is 64 keV and Swank *et al.*'s (1977) value $L_X = 9 \times 10^{32} D_{100}^2$ erg/s for the 2–60 keV luminosity in an optical high state represents essentially all of the X-ray emission escaping the system. Thus we need a case (a) solution (to get the observed X-ray temperature $T_e \approx T_s$) in which $L_{ff} = 2L_X = 1.8 \times 10^{33} D_{100}^2$ erg/s. The *emitted* cyclotron luminosity of the weak pole is again of order $(1–3) \times 10^{32} D_{100}^2$ erg/s, so we require $6 \lesssim a \lesssim 18$. Taking first $B_8 = 0.4$ and $m_* = 5$, a value $a = 6$ leads from Fig. 2 to point W, where $F_{16} = 1.8$, $\phi = 3.0$ and $L_{ff} = 4.1 \times 10^{33}$ erg/s. Hence W is an acceptable representation of the weak pole provided $L_{ff}/L_{cyc} \approx 6$ and the distance of the system is of order 150 pc. Larger values of a imply, keeping $B_8 = 0.4$, that F_{16} is higher than its value 1.8 at W, leading to larger predicted L_{ff}'s which require the distance to the system to be greater. Thus for $a = 10$, $B_8 = 0.4$ gives $F_{16} = 2.66$, or $L_{ff} = 6.4 \times 10^{33}$ erg/s; this requires the distance to the system to be ~190 pc. In all cases a photoelectric cut-off $\tau_{pe} = 1$ should appear at about 3 keV in the X-ray spectrum: this agrees quite well with Swank *et al.*'s (1977) inferred hydrogen column density $N_H = 3 \times 10^{22}$ cm^{-2} ($\tau_{pe} = 1$ for ~2.5 keV). Moreover, for all of these solutions we find D/R of order 0.1, so that the two-pole model is self-consistent. If instead of the above B_8, m_*, we take $B_8 = 0.25$, $m_* = 8$, then $a = 6$ leads to $F_{16} = 1.8$, $L_{ff} = 4.1 \times 10^{33}$ erg/s requiring a distance of 150 pc as before. All other quantities, including the X-ray cut-off energy, are very similar to the values for the $a = 6$, $B_8 = 0.4$ solution above, except that $\phi \approx 2$ rather than 3. For $B_8 = 0.25$, $a = 10$, we are, however, forced to put the system at a distance of 210 pc in order to reconcile the predicted and observed X-ray luminosities. To summarize: provided cyclotron radiation is not less than about one-sixth of bremsstrahlung, good fits to all observed quantities are obtained if the distance to the system is about 150 pc, irrespective of whether m_* is chosen to be 5 or 8 in equation (24). The solution with $m_* = 5$ has the merit of not requiring very dissimilar magnetic field strengths ($B_8 = 0.4, 0.7$) at the two poles; the accretion rates on to the two poles are of order 10^{16} and 10^{15} g/s respectively for all acceptable solutions.

So far we have considered only observations of AM Her in an optical high state ($V \sim 12.8$). The predicted behaviour as the optical luminosity varies is best understood using Fig. 3, which is the $\log F$–$\log B$ plane with $m_* = 5$, $M_1 = 1$, $R_9 = 0.53$, i.e. the same as Fig. 2, but with the curves L_{ff} = constant, L_{cyc} = constant, particularly emphasized. (The latter curves are easily worked out from the former.) What is very noticeable is that the curves L_{cyc} = constant are almost vertical in region (a), and effectively horizontal in region (b). A variation of the accretion rate simply causes the system point to move up and down the vertical line $B_8 = 0.4$. Hence the following predictions result immediately:

(1) For an optical high state (system point near W), changes by factors ~2 or more in F do not alter L_{cyc}. Thus the X-ray luminosity ($\propto F$) can vary appreciably while the optical luminosity is unchanged.

(2) In order to reduce L_{cyc} significantly one must move the system point into the case (b) region of the diagram; here L_{ff} is small, so in the optical low states ($V \sim 14.8$) there should be little or no hard ($\geqslant 2$ keV) X-ray emission.

If we consider the strong pole, a diagram qualitatively exactly like Fig. 3 can be constructed, with the system point lying in region (b) (*cf.* Fig. 1). In this region $L_{cyc} \propto F$, so as the accretion rate on to this pole rises and the system point moves towards its highest

position (S on Fig. 1) its optical luminosity should rise significantly. This contrasts with the behaviour of the weak pole where, as we have seen, once case (a) conditions obtain there is little change in optical brightness. It is reasonable to assume that the accretion rates on to each pole rise and fall together (although a precise relationship is of course difficult to estimate), giving a third prediction:

(3) During the rise to optical maximum the optical brightness of the strong pole should increase rather more rapidly than that of the weak; hence the optical secondary minimum should tend to get shallower during the optical rise or even disappear at optical maximum.

All the predictions (1)–(3) appear to be supported by the available observational evidence. During the period 1974 November to 1978 May AM Her was detected frequently by the Leicester Sky Survey Instrument on *Ariel V*. There is considerable variability (~ 2×)

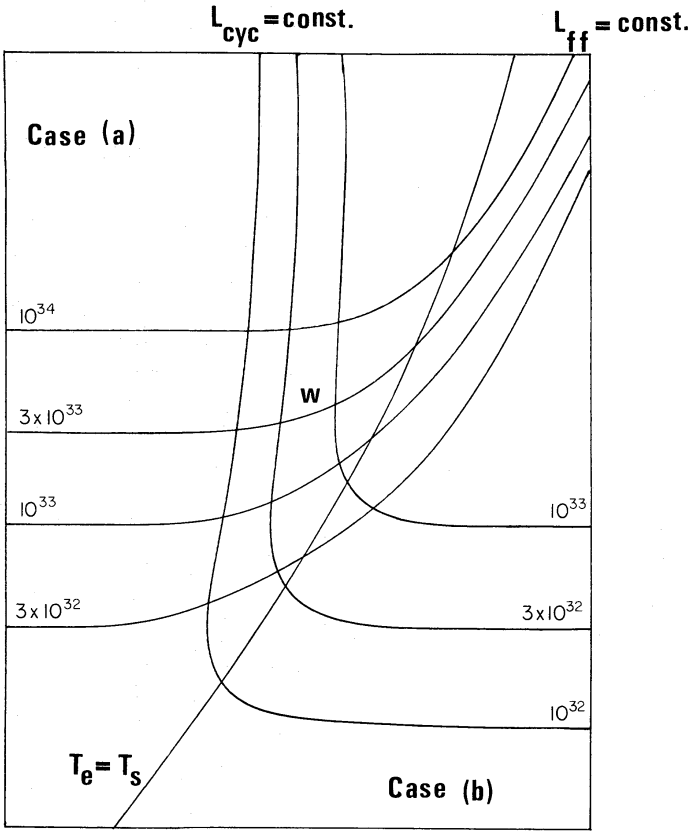

Figure 3. Log F–log B diagram with exactly the same parameters as Fig. 2, but with the curves L_{ff} = constant, L_{cyc} = constant, emphasized. Point W represents the weak-pole solution of Fig. 2. As the accretion rate varies, the system point moves up and down the vertical lines $B = 4\times10^7$ G. In an optical high state the system point is near W, and changes in F by factors ~ 2 or more do not alter L_{cyc}, as the curves L_{cyc} = constant are themselves almost vertical near W. Thus in an optical high state, F, and in consequence the X-ray emission, can vary appreciably without changing the optical luminosity, as observed. Furthermore, to reduce the optical luminosity ($\sim L_{cyc}$) significantly F has to be so low that the system point crosses the curve $T_e = T_s$; here L_{ff} is small, and hence little or no hard X-ray emission is expected in optical low states. This conclusion is again supported by observation. A diagram qualitatively the same as Fig. 3 can be constructed for the strong pole (parameters of Fig. 1), except that the system lies *below* the curve $T_e = T_s$ (*cf.* Fig. 1). In this region $L_{cyc} \propto F$, so an increase in F causes a significant rise in optical brightness of this pole, in contrast with the situation for the weak pole. Thus if the accretion rates on to the two poles rise and fall roughly in step the optical brightness of the strong pole should increase more rapidly than that of the weak pole during the rise to optical maximum. This accounts for the observed decrease in optical secondary minimum during such a rise.

in the 2–10 keV count rate, but at all detections the system was at optical maximum $V \sim 12.8$ (M. G. Watson, W. Krzemiński, private communications), supporting (1) and (2). All other hard X-ray sightings of AM Her we have been able to find in the literature were also made at optical maximum. The behaviour predicted in (3) was observed by Priedhorsky & Krzemiński (1978).

In concluding this section we should mention the balloon-borne observation of Staubert *et al.* (1978) which appears to require a much softer ($kT_e \approx 18$ keV) bremsstrahlung X-ray spectrum. The total luminosity implied by this spectrum is $L_X \approx 4 \times 10^{32} D_{100}^2$ erg/s, or an emitted $L_{ff} \approx 8 \times 10^{32} D_{100}^2$ erg/s. This is certainly larger than the cyclotron luminosity of the X-ray emitting (weak) pole: hence an attempt to find the parameters of this pole demands a case (a) solution. Since in case (a) $T_e = T_s$, a shock temperature $kT_s \approx 18$ keV is required, which from fig. 1 of Fabian *et al.* (1976) leads to a white dwarf mass M near $0.5 M_\odot$. An independent determination of M and confirmation of the above result would give a test of the basic shocked accretion-flow model.

4 Soft X-ray emission from AM Her

AM Her is a soft X-ray source in both high and low optical states, e.g. Hearn, Richardson & Clark (1976), Bunner (1978) and Tuohy *et al.* (1978). In the latter observation, the flux in the range 0.15–0.5 keV implied a luminosity $\approx 9 \times 10^{32} D_{100}^2$ erg/s, about the same as Swank *et al.*'s (1977) 2–60 keV flux, both observations being made during an optical high state. The soft X-ray spectrum can be fitted by either a blackbody or thermal bremsstrahlung spectrum, with in both cases a low-energy photoelectric turnover, corresponding to a hydrogen column density $N_H \approx 3 \times 10^{20}$ cm^{-2} (Tuohy *et al.* 1978). The near identity of the soft and hard X-ray light curves, each showing a single deep eclipse at the same binary phase, means that the emissions come from the neighbouring regions. (In the two-pole slow rotator models these must of course be near the weak pole.) Since, however, the column density N_H for the soft X-rays is only ~ 1 per cent of that for the hard X-rays, the regions are not identical; indeed the N_H for the soft X-rays is about what would be expected from interstellar absorption at the suggested distance $D_{100} \sim 1$ of the system. Hence the soft X-ray region probably 'surrounds' the site of hard X-ray emission, and it is natural to suppose that the origin of the soft X-ray flux is emission from an accretion column, absorbed and re-radiated in some thermalized form by the white dwarf atmosphere. Since one-half of the accretion luminosity is emitted 'downwards' from each accretion column and is therefore intercepted by the white dwarf in this way, there is certainly sufficient power available to supply the observed flux. In order to check this idea we must consider the possible spectra of the re-emitted radiation.

The simplest hypothesis for this luminosity is total thermalization, i.e. that it has a blackbody spectrum. To estimate the temperature T_b parametrizing this spectrum we need an idea of the area A from which it is emitted; then T_b follows from demanding

$$A\sigma T_b^4 = \tfrac{1}{2} L_{acc}. \tag{24}$$

For $D \ll d$, the area $A \approx \pi d^2$, while for $D \gg d$ an upper limit to T_b is given by assuming that most of the intercepted radiation is re-emitted from an area $A \approx \pi D^2$ of the white dwarf's surface. Thus we may take

$$A \approx \pi(d + D)^2 = \frac{\pi}{4} d^2(\phi + 1)^2$$

in general. Using the definition of f' we find $A \approx \pi R^2 f'(\phi + 1)^2$. Now from equation (24) we

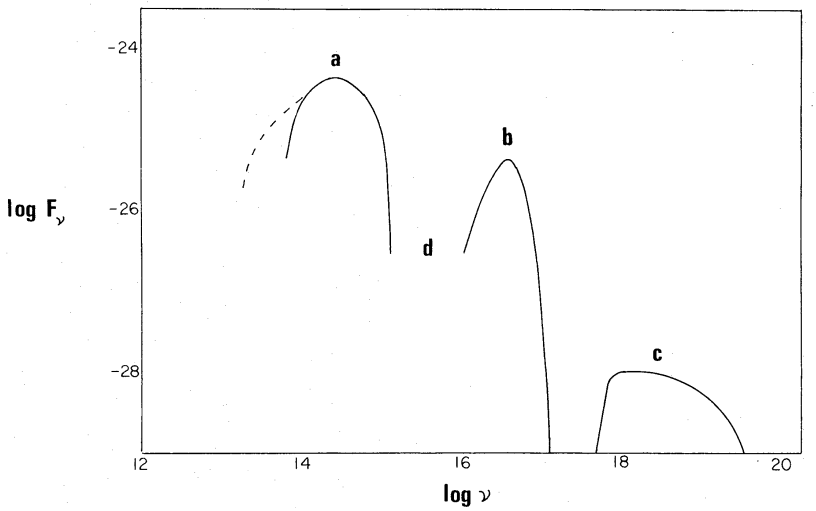

Figure 4. Idealized spectrum of the weak pole of AM Her, with a distance of 100 pc assumed and F_ν measured in erg s^{-1} cm^{-2} Hz^{-1}. Key to curves: (a) Infrared and optical radiation due to self-absorbed cyclotron emission from shock-heated electrons. Infrared light curves at wavelengths longer than 2.2 μm are necessary to determine the width of the cyclotron 'line'. The solid curve shows the emission for the parameters adopted in the paper, while the dotted curve indicates that a broader cyclotron spectrum is possible. For wavelengths $\gtrsim 30\,\mu$m there is probably only weak emission from the accretion columns of the white dwarf, with $F_\nu \lesssim 10^{-27}$ erg s^{-1} cm^{-2} Hz^{-1}. (b) Soft X-ray and far UV emission from the part of the white dwarf atmosphere heated by hard X-rays from the accretion column (the effect of interstellar absorption is not shown). Region d of the spectrum of the weak pole is probably dominated by line emission from part of the atmosphere. (c) Hard X-rays due to bremsstrahlung emission by the shock-heated electrons (a shock temperature $kT_s = 60$ keV has been assumed). The low energy end (~ 3 keV) of this spectrum shows the effect of photoelectric absorption in the cooler part of the accretion column above the shock. (d) See (b) above. It should be emphasized that this spectrum refers only to emission from the weak pole itself, which is therefore periodically eclipsed, as observed in light curves for regions a, b, c. In region d for example, there may be emission from gas further out from the white dwarf which is not eclipsed, and indeed the U curve appears different in form to the other light curves. In the spectrum of the strong pole, features b and c are absent, while a is somewhat stronger, turning down at about 1.5 μm.

can get T_b: for our purposes it is useful to find the curves T_b = constant in the log F–log B plane. We find

$$F_{16} = 2.48 \times 10^{-31} T_b^{28/5} B_8^{-4/5} M_1^{-6/5} R_9^{16/5} (\phi + 1)^{14/5}.$$

The curve $T_b = 2.8 \times 10^5$ K corresponding to the lower of Tuohy *et al.*'s (1978) extreme values deduced for T_b from observation, is plotted on Fig. 2. Even in the high state the weak pole, which from the light curves has to be the seat of soft X-ray production, lies somewhat below the lower value of T_b at W. We find a very similar result for other possible values of m_*. Since we have if anything probably overestimated T_b, this means that the blackbody hypothesis is difficult to sustain using the present approach. We believe, however, that the soft X-rays are likely *not* to have a blackbody spectrum, for the reasons detailed below.

If we use the limits $2.8 \times 10^5 < T_b < 4.6 \times 10^5$ on the blackbody temperature, the 0.15–0.5 keV soft X-ray window of *HEAO-1* (the widest used in observations of AM Her) accepts between 12 and 46 per cent of the total blackbody flux from the object, the larger figure applying to the higher temperature. Thus the total blackbody emission from AM Her is of order $8L_{soft}$ (or $2L_{soft}$) where L_{soft} is the observed soft X-ray luminosity; this must represent about one-half of the accretion luminosity of the weak pole, so that we require $L_{acc} \sim 16 L_{soft}$ ($4L_{soft}$). The other half of the accretion luminosity must appear as cyclotron or hard X-ray emission, but the amount involved (8 or $2L_{soft}$) is embarrassingly large; the

observed total of these two kinds of emission from the weak pole is no more than about $1.2L_{\rm soft}$. Thus the unobserved cyclotron or hard X-ray luminosity is $\sim 7L_{\rm soft}$ ($\sim L_{\rm soft}$). If this luminosity appears as hard X-rays, it must do so above 60 keV to escape observation. This immediately demands a white dwarf mass near the Chandrasekhar limit in order to raise the shock temperature sufficiently, leading, in the two-pole slow rotator models at least, to the severe difficulties for the strong pole mentioned in Section 3. If instead we try to put this excess luminosity into cyclotron radiation (e.g. Tuohy *et al.* 1978) we also run into difficulties. First, the observed lack of polarized emission at wavelengths shorter than 4000 Å (see Kruszewski (1978) for details and references) make the presence of strong cyclotron emission in the ultraviolet improbable. Similarly, if the excess luminosity is to appear at infrared wavelengths the magnetic field, at least at the weak pole, must be considerably less than usually assumed. In any case, putting the excess luminosity into $L_{\rm cyc}$ means that a case (b) solution is required for the weak pole. Hence to get a bremsstrahlung temperature of $\gtrsim 60$ keV we must again have the white dwarf mass near the Chandrasekhar limit, with the attendant difficulties referred to earlier.

An alternative to the blackbody hypothesis is to assume that the soft X-rays are due to hard X-rays from the accretion column being degraded and partially reflected by scattering in the white dwarf atmosphere, together with optically thin emission from the parts of the atmosphere heated by this process. The 0.15–0.5 keV spectrum would then be the Wien tail expected from Comptonization of the hard X-rays, and most of the inferred soft X-ray luminosity would actually appear in the observing window, avoiding the problems encountered above. In view of the complicated spectrum expected from optically thin gas at the temperatures ($\lesssim 5\times 10^5$ K) likely from observation, plus the difficulty of the radiative transfer problem in the (probably highly inhomogeneous) emission region, it is clear that more work is needed on models for the soft X-ray component. Fig. 4 represents an idealized picture of the spectrum of the weak pole of AM Her.

5 Conclusions

In this paper we have developed a quantitative theory of accretion on to highly magnetized white dwarfs and applied it to AM Her. The theory enables us to deduce parameters for the system in an optical high state which provide acceptable fits to all observed quantities. The detailed time variation of the system is also correctly predicted by this theory. The direct correlation between X-ray and optical luminosity in AM Her contrasts with the directly anticorrelated behaviour in SS Cyg (Ricketts *et al.* 1979). This difference occurs for two main reasons: first, in SS Cyg most of the optical light comes from the disc, while in AM Her we believe it is due to cyclotron radiation. Secondly, in AM Her the accretion rate is fairly modest ($F_{16}\lesssim 1$) by comparison with SS Cyg ($4\lesssim F_{16}\lesssim 2\times 10^3$), so that in the latter system X-rays are always produced, but are cut off at maximum light by absorption within the system.

We believe that the considerations of the present paper provide support for the two-pole slow rotator model for AM Her, in particular in the version put forward by Kruszewski (1978), although other models are not ruled out. One might also try to apply the present approach to the similar systems VV Puppis and AN Ursae Majoris. These are not known to be hard X-ray emitters, and the present observational data are probably rather too sparse to allow a quantitative discussion. If we consider these objects as a class, it seems clear that their relatively high magnetic fields pick them out from other cataclysmic variables. The possibility naturally arises of AM Her-type behaviour at infrared wavelengths from systems with weaker fields. We shall discuss this question in a subsequent paper.

Theoretically, the most serious defect in the present theory is the lack of a good understanding of the self-absorbed cyclotron emission. The semi-empirical approach used here does fit in with the rather crude considerations available at the moment in that the deduced m_* values do appear to correlate with the accretion rates F correctly: a higher F means larger opacity in the accretion columns and consequently a higher m_*. However, the quantitative agreement with theoretically predicted m_* values is not good and this aspect clearly needs further study.

Acknowledgments

We would like to thank M. G. Watson for providing and discussing *Ariel V* data and W. Krzemiński for communicating optical results. Remarks by a referee were helpful in improving the presentation of the paper. During the writing of this paper JPL held a SRC Senior Visiting Fellowship.

References

Aizu, K., 1973. *Prog. Theor. Phys.*, **49**, 1184.
Angel, J. R. P., 1978. *A. Rev. Astr. Astrophys.*, **16**, 487.
Bunner, A. N., 1978. *Astrophys. J.*, **220**, 261.
Chanmugam, G. & Wagner, R. L., 1978. *Astrophys. J.*, **222**, 641.
Fabian, A. C., Pringle, J. E. & Rees, M. J., 1976. *Mon. Not. R. astr. Soc.*, **175**, 43.
Fabian, A. C., Pringle, J. E., Rees, M. J. & Whelan, J. A. J., 1977. *Mon. Not. R. astr. Soc.*, **179**, 9P.
Fabbiano, G., Gursky, H., Schwartz, D. A., Schwartz, J., Bradt, H. V. & Doxsey, R. E., 1978. *Nature*, **275**, 721.
Hearn, D. R., Richardson, J. A. & Clark, G. W., 1976. *Astrophys. J.*, **210**, L23.
Hoshi, R., 1973. *Prog. Theor. Phys.*, **49**, 776.
Jameson, R. F., Akinci, R., Adams, D. J., Giles, A. B. & McCall, A., 1978. *Nature*, **271**, 334.
Katz, J. I., 1977. *Astrophys. J.*, **215**, 265.
King, A. R., Ricketts, M. J. & Warwick, R. S., 1979. *Mon. Not. R. astr. Soc.*, **187**, 77P.
Kruszewski, A., 1978. *Nonstationary Evolution of Close Binaries*, p. 55, ed. Żytkow, A. N., PWN, Warsaw.
Kylafis, N. D. & Lamb, D. Q., 1979. *Astrophys. J.*, submitted.
Mason, K. O., Lampton, M., Charles, P. & Bowyer, S., 1978. Preprint.
Masters, A. R., Pringle, J. E., Fabian, A. C. & Rees, M. J., 1977. *Mon. Not. R. astr. Soc.*, **178**, 501.
Neugebauer, G., Werner, M., Priedhorsky, W. C. & Krzemiński, W., 1979. *Astrophys. J.*, in press.
Priedhorsky, W. C. & Krzemiński, W., 1978. *Astrophys. J.*, **210**, 597.
Ricketts, M. J., King, A. R. & Raine, D. J., 1979. *Mon. Not. R. astr. Soc.*, **186**, 233.
Staubert, R., Kendziorra, E., Pietsch, W., Reppin, C., Trümper, J. & Voges, W., 1978. *Astrophys. J.*, **225**, L113.
Stockman, H. S., Schmidt, D., Angel, J. R. P., Liebert, J., Tapia, S. & Beaver, E. A., 1977. *Astrophys. J.*, **217**, 815.
Swank, J., Boldt, E., Holt, S. & Serlemitsos, P., 1979. *Astrophys. J.*, submitted.
Swank, J., Lampton, M., Boldt, E., Holt, S. & Serlemitsos, P., 1977. *Astrophys. J.*, **216**, L71.
Tapia, S., 1976. *IAU Circ. No. 2987.*
Tapia, S., 1977. *Astrophys. J.*, **212**, L125.
Tuohy, I. R., Lamb, F. K., Garmire, G. P. & Mason, K. O., 1978. *Astrophys. J.*, **226**, L17.
Watson, M. G., Sherrington, M. R. & Jameson, R. F., 1978. *Mon. Not. R. astr. Soc.*, **184**, 79P.

Appendix

In this Appendix we give reasons for the choice of f' used in the paper. If we suppose the white dwarf rotates synchronously with one magnetic pole facing the secondary, there will be some characteristic radial distance r_0, measured from the centre of the white dwarf, at which the accreting matter begins to flow down the magnetic field lines on to the poles of the white dwarf. We suppose that at r_0 the body of the matter subtends a half-angle α at

the white dwarf, which implies a solid angle $\Omega \sim \pi \sin^2 \alpha$. Equating kinetic and magnetic energy densities at r_0, we have

$$\rho c^2 \sim \frac{B^2}{8\pi}\left(\frac{R}{r_0}\right)^6$$

where ρ is the matter density at r_0, c the local sound speed and B the magnetic field at the surface $r = R$ of the white dwarf. If instead we had spread the same amount of matter out over a full sphere at r_0 the density would have been ρ', where $\rho = (4\pi/\Omega)\,\rho'$. If we define a spherical Alfvén radius R_A (e.g. Stockman *et al.* 1977) by

$$\rho' c^2 = \frac{B^2}{8\pi}\left(\frac{R}{R_A}\right)^6$$

we find

$$r_0 = \sqrt[6]{\frac{\Omega}{4\pi}}\,R_A.$$

Taking the equation of a field line in polar coordinates at $r = C \sin^2 \theta$, with C a constant, yields

$$C = \frac{R_A}{(4)^{1/6} \sin^{5/3} \alpha}$$

for the value of C on this 'limiting' field line. Thus at $r = R$ on this field line,

$$\sin^2 \theta = \frac{R}{C} = \frac{R}{R_A}(4)^{1/6} \sin^{5/3} \alpha.$$

Hence the fraction of the white dwarf's area over which accretion takes place is

$$f' = \frac{\pi R^2 \sin^2 \theta}{4\pi R^2} = \frac{1}{(4)^{5/6}}\frac{R}{R_A}\sin^{5/3} \alpha,$$

$$\approx f_{\rm sph} \sin^{5/3} \alpha,$$

where $f_{\rm sph} = R/2R_A$. We expect $\sin^{5/3} \alpha \sim \frac{1}{2}$ for AM Her and similar systems, since (r_0, α) will be quite close to but outside the secondary's Roche lobe, which yields $\sin^{5/3} \alpha$ of this order for reasonable mass ratios. Thus $f' \sim \frac{1}{2} f_{\rm sph}$, and the expression for $f_{\rm sph}$ given by Fabian *et al.* (1976) gives the formula for f' used in this paper.